Genetic Algorithm Optimization of a Dual Polarized Concentric Ring Array

Pedro Mendes Ruiz [1], Israel D. Hinostroza Sáenz [1], Régis Guinvarc'h [1], and Randy Haupt [2]

[1] SONDRA
CentraleSupélec, Gif-sur-Yvette, 91190, France
{pedro.mendesruiz, israel.hinostroza, regis.guinvarch}@centralesupelec.fr

[2] Electrical Engineering and Computer Science
Colorado School of Mines, Golden, CO 80401, USA
rhaupt@mines.edu

Abstract — We use a genetic algorithm to minimize the relative sidelobe level (RSLL) of a dual polarized concentric ring array. The optimization variables are the placement of uniformly weight spiral antennas in an aperture with a small area. We optimized a cost function with isotropic sources instated of spiral elements to make the cost function reasonable to evaluate. We developed approaches to calculate a faster cost function and reduce the number of function calls in the optimization. We then calculated the array with an approximation of the element pattern to evaluate its performances.

Index Terms — Concentric ring array, genetic algorithms, optimization, phased array, planar array, spiral antenna, wideband array.

I. INTRODUCTION

Dual circularly polarized wideband arrays find use in several applications, including weather radar [1] and synthetic aperture radar [2]. As in [3], the array design in this paper has a bandwidth from 1 to 2 GHz with a maximum scan angle of 30°. The bandwidth is defined by a reflection coefficient smaller than -10 dB, dual circular polarization with an axial ratio smaller than 3 dB, and a relative sidelobe level smaller than -10 dB. Two-arm center-fed spiral antennas [4] are excellent elements for this application, because they are very wideband, conformal and circularly polarized. Dual polarization is possible by interleaving spirals of opposite polarization [5], [6]. A dual polarized concentric ring array was developed using two-arm center-fed Archimedean spirals as the radiating element with each ring of spirals backed by a cavity. To ensure a good axial ratio, we use the sequential rotation technique [7]. Non-uniformly spaced concentric rings mitigate the sidelobes [6]. In [3] we added a size constraint to the optimization to reduce the size of the array. This work expands on the paper presented at the ACES 2017 conference in Florence [8]. The goal of the genetic algorithm optimization [9] described in this work is to find a smaller array than in

[6] with a similar bandwidth by optimizing the rings positions using the size constraint in [3].

II. CONCENTRIC RING ARRARY

A diagram of the concentric ring array, which has $N_r = 4$ rings, appears in Fig. 1. Variables in the i-th ring design ($i = 0, ..., N_r - 1$) include the ring spacing Δ_i and the ring rotation Φ_i. The array consists of Archimedean spirals with a diameter of $D_{spi} = 10.5$ cm and a lower cut-frequency of 1 GHz [6]. The spacing between elements of the same polarization within a ring has an approximate value of $d_{elem} = 24.34$ cm [6]. Every other element in a ring is RH (right hand) polarized, while the others are LH (left hand) polarized. The array is modeled using isotropic point sources for the optimization.
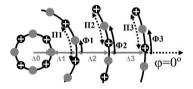

Fig. 1. Concentric ring array: filled and cross circles represent RH and LH polarized spirals, respectively.

The number of spirals of the same polarization (N_i) in a ring of radius r_i is determined by:

$$N_i = \left\lfloor \frac{2\pi r_i}{d_{elem}} \right\rfloor, \tag{1}$$

where $\lfloor x \rfloor$ is the floor function. We can then calculate the angular distance between two elements of the same polarization as follows:

$$\Pi_i = \frac{2\pi}{N_i}. \tag{2}$$

For the optimization, the values of the ring rotations are restricted to $0 \le \Phi_i \le \Pi_i$ and the array radius is limited by a maximal value $R_{max} = 1.3$m [3]. This optimization results in an array with a radius close to the maximum allowed. The surface area obtained in that case is equivalent to 42% of that in [6], similar to [3].

III. ONE RING ARRAY

As our final goal is to minimize the RSLL of the concentric ring array at all frequencies, we first look at the array factor (AF) at the highest frequency in the bandwidth, 2 GHz. In order to consider all steering directions up to θ_s, we will look at the u-v space in the region:

$$u^2 + v^2 \leq (1 + \sin\theta_s)^2. \tag{3}$$

In Fig. 2 we show the AF of a one ring array calculated at 2 GHz inside the region defined by $u^2 + v^2 \leq 1.5^2$, which contains all the sidelobes that can appear in the visible zone at 2 GHz for a maximal steering of $\theta_s = 30^o$. By looking at the AF with the u-v axes normalized by d_{elem}/λ, we observe high sidelobes in the rings with an integer radius, corresponding to the grating lobe regions. In the concentric ring array we should expect to have the larger sidelobes appearing in those regions.
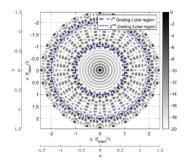

Fig. 2. Array Factor of a one ring array with a radius of 1.085 m and 28 elements uniformly spaced, showing all sidelobes that appear in the visible zone at 2 GHz for a maximal steering of $\theta_s = 30^o$. The u-v axes are shown for the AF at 2 GHz, as well as the axis normalized by d_{elem}/λ. The 1st (dashed) and 2nd (dotted) Grating Lobe (GL) regions are highlighted in the Array Factor.

IV. ARRARY BANDWIDTH

The isolated spirals used in this array have a reflection coefficient higher than -10 dB for frequencies below 1 GHz, so this is used as the lower limit of the bandwidth. In order to calculate the higher limit of the bandwidth of the array, we used a mean radiated element model to find the total radiated field, and then find the RSLL, that should be smaller than -10 dB [6].

To obtain an approximation of the embedded element pattern, which we will call $\boldsymbol{E}_{model}$, we simulated a small one ring array in FEKO. The array had 8 spiral elements (4 per polarization) backed by a cavity [6], and we simulated it with one of the spirals being excited with a voltage source and the other 7 spirals were adapted with 220 Ω loads. In order to calculate the array pattern with the spiral elements and using the sequential rotation technique, we first calculated the radiated field of each of the rotated elements:

$$\boldsymbol{E}_{el_{ji}} = rotation\left(\boldsymbol{E}_{model}, \alpha_{rot_{ji}}\right), \; \alpha_{rot_{ji}} = \pm\gamma_{ji}, \tag{4}$$

where γ_{ji} is the angular position of the j-th element in the i-th ring of the array, having a positive value for the LH polarized elements and a negative value for the RH polarized elements. Then, we summed the radiated fields, multiplying each of them by the corresponding sequential rotation phase $\alpha_{rot_{ji}}$ as well as the steering phase and the positioning phase, $\delta_{pos_{ji}}$:

$$\boldsymbol{E}(\varphi,\theta) = \sum_{i=0}^{N_r-1} \sum_{j=1}^{N_i} e^{-j\delta_{pos_{ji}}} e^{-j\alpha_{rot_{ji}}} \; \boldsymbol{E}_{el_{ji}}(\varphi,\theta), \tag{5}$$

$$\delta_{pos_{ji}} = \frac{2\pi}{\lambda}\left(x_{ji}(u-u_s) + y_{ji}(v-v_s)\right), \tag{6}$$

with N_i being the number of elements in the i-th ring. x_{ji} and y_{ji} are the positions of the j-th element in the i-th ring. u and v are the observation direction in the u-v space. u_s and v_s are the steering directions in the u-v space.

V. GENETIC ALGORITHM OPTIMIZATION

A. First optimization: Optimizing all sidelobes

The goal of the optimization is to minimize the RSLL in the desired bandwidth (1-2 GHz), considering a maximum steering of θ_s=30°. In order to find the maximum sidelobe level, the array pattern was calculated, at 2 GHz, in the region defined by $u^2 + v^2 \leq 1.5^2$ (equation 3). The cost function analyzes that region and returns the highest RSLL in dB.

Table 1: Optimization optimal values

	Δ0 (cm)	Δ1 (cm)	Δ2 (cm)	Δ3 (cm)	Φ1 (rad)	Φ2 (rad)	Φ3 (rad)
1st Opt.	46.81	28.92	27.86	27.77	0.0467	0.0784	0.1399
2nd Opt.	46.53	27.07	28.25	29.84	0.1319	0.0895	0.0562
3rd Opt.	47.00	26.62	30.05	27.96	0.0871	0.2416	0.1452

The genetic algorithm had a population size of 200 and ran for a maximum of 200 generations. A single function call for a concentric ring array of isotropic point sources took between 3.8 and 6.3 s. The whole optimization took 38 hours to finish using 4 cores, with a mean of 55 generations before reaching the stop criterion for each of the eight genetic algorithm iterations and a total of 88985 evaluations of the cost function. The optimization results can be seen in Table. 1. Figure 3 shows the optimized array pattern in u-v space at 2 GHz. Figure 4 is the u-cut of the Array Factor that has the highest sidelobes. We note that the RSLL stays bellow -11dB for scanning up to 30° and a frequency up to 2 GHz with a maximum radius of 1.3m. We also note that there are two groups of high sidelobes in the regions corresponding to the grating lobe regions, as we expected from the results in Section III. In Fig. 5 we plot the RSLL of the optimized array using the method presented in Section IV, which resulted in a bandwidth from 1-1.3 GHz (27% of [6]). To better explain

what is happening in the array pattern, we will look at the radiated field of the steered array at 2 GHz (Fig. 6). We observe that the 1st ring of grating lobes is getting larger while the 2nd ring of grating lobes is being attenuated.
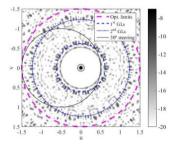

Fig. 3. Array factor of the array obtained from the 1st optimization at 2 GHz. In thick dashed pink we have the limits of the sidelobe search for the optimization cost function. In thin dashed blue and dottted blue, we have the 1st and 2nd grating lobe regions, respectively. In black we have the visible zone once steered to $[\theta_s, \phi_s] = [30°, 0°]$.
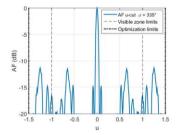

Fig. 4. Array factor representative u-cut ($\phi = 335°$) for the concentric ring array optimized at the $\theta_s < 30°$ zone, at 2 GHz (1st optimization).

B. Second optimization: Avoiding 2nd GLs

By taking into account this reduction in the 2nd grating lobes, we decided to re-optimize the array, changing the optimized region in the AF to exclude those sidelobes, so the 1st grating lobes are prioritized and thus further reduced, which compensates the increase they get when we steer the array.

Now, the optimized region of the sidelobes in the AF at 2 GHz is defined by $u^2 + v^2 \leq 1.15^2$, which corresponds to $(u \, d_{elem}/\lambda)^2 + (v \, d_{elem}/\lambda)^2 \leq 1.866^2$ by normalizing as in section III and includes all sidelobes until just before the 2nd grating lobe region. By using the same optimization procedure as in section V-A, we got the results presented in Table 1. A single cost function call took between 2.2 and 3.7 s, 59% of the time required by the cost function in section V-A, which happens because less points are being computed in the u-v space.

The whole optimization took 21 hours to finish using 4 cores, with a mean of 48 generations before reaching the stop criterion for each of the eight genetic algorithm iterations and a total of 77988 evaluations of the cost function. In Fig. 7 we show the AF of the optimized array

and, in Fig. 8, two u-cuts of that AF representative of the sidelobe level. We can see from the figures that the new optimization was able to further reduce the prioritized sidelobes by relaxing the constraints on the sidelobes appearing in the 2nd GL region. In Fig. 5 we show the RSLL calculated via the method in section IV, and we observe that the bandwidth was successfully increased to 1-2 GHz (95% of [6]).
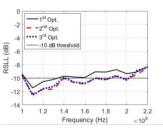

Fig. 5. RSLL in function of frequency of the 1st (continuous black), 2nd (dashed red) and 3rd (dotted blue) optimized array using the method described in Section IV.
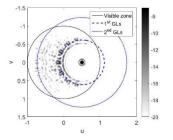

Fig. 6. Electric field of the array obtained from the 1st optimization with a steering of $[\theta_s, \phi_s] = [30°, 0°]$, calculated using the method from section IV, in the u-v space. In continuous black we have the visible zone. In dashed blue and dottted blue, we have the 1st and 2nd grating lobe regions, respectively.

C. Third optimization: using only half of the AF

Finally, we noticed that by optimizing the sidelobes in half of the u-v space, we got very similar results while significantly reducing the computation time. The optimization was repeated with the new cost function with the results presented in Table 2. The cost function evaluation time reduced to 1.1-1.9 s, 30% of the time required in section V-A. The whole optimization took 8 hours to finish using 4 cores, with a mean of 36 generations before reaching the stop criterion for each of the eight genetic algorithm iterations and a total of 59387 evaluations of the cost function. The resulting AF is similar to that obtained in the 2nd optimization (Fig. 7). In Fig. 5 we show the RSLL calculated via the method from Section IV. The resulting RSLL is so similar to that from the array of the 2nd optimization that their curves are almost superposed, showing that limiting the optimized zone to half of the u-v space is a good approach to reduce the computation time. Further reducing the optimized zone created an imbalance in the sidelobes of the

optimized array, resulting in larger sidelobes for the worst case scenario.
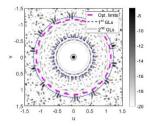

Fig. 7. Array factor of the array obtained from the 2nd optimization at 2 GHz. In thick dashed pink we have the limits of the sidelobe search for the optimization cost function. In thin dashed blue and dottted blue, we have the 1st and 2nd grating lobe regions, respectively.
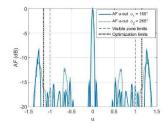

Fig. 8. Array factor representative u-cuts ($\phi_1 = 165°$ and $\phi_2 = 265°$) for the concentric ring array optimized at the $(u\, d_{elem}/\lambda)^2 + (v\, d_{elem}/\lambda)^2 \le 1.866^2$ zone, at 2 GHz (2nd optimization).

VI. RESULTS DISCUSSION

By using three criteria for defining the array bandwidth, we have shown that limiting the optimized zone of the AF to exclude the 2nd GL zone is a good strategy for reducing the optimization time. The sidelobes in the 2nd GL zone are attenuated once the radiating pattern of the array's elements are taken into account. Prioritizing the sidelobes in the 1st GL zone when optimizing the array's AF compensates their rise once the radiating pattern is considered. By optimizing only half of the u-v space there was no bandwidth reduction, proving it to be a great way to reduce the computation time of the cost function. Further reduction of the optimized region consistently caused a reduction in the bandwidth, so it was not considered in this paper. As for the time reduction, there are two main factors. First, by limiting the optimized zone in the AF, there are less points to be computed in the u-v space, which results in a faster cost function. This is true for both the 2nd and 3rd optimizations. Second, in the 2nd and 3rd optimizations the genetic algorithms converged faster. We cannot draw any special conclusions from this faster convergence as we would need to validate that fact by re-optimizing the array enough times to have statistically meaningful results, which was time prohibitive in our case. By comparing the first and last optimizations, the latter spent 22.3% of the time needed for the first one while enhancing the bandwidth from 27% to 95% (1-2 GHz) of [6].

Table 2: Comparison of results

Optimized zone	$\theta_s < 30°$ at 2 GHz	Avoid 2nd GL	Avoid 2nd GL, $u > 0$
Bandwidth (GHz)	1-1.3 (27%)	1-2 (95%)	1-2 (95%)
Cost function call time (s)	3.8-6.3 (100%)	2.2-3.7 (59%)	1.1-1.9 (30%)
Cost function calls	88985 (100%)	77988 (88%)	59387 (67%)
Opt. time (h)	38 (100%)	21 (55%)	8 (22%)

VII. CONCLUSIONS

By analyzing the concentric ring array topology with a size constraint [3] and redesigning its cost function, it was possible to find an array with 95% of the bandwidth in [6] and 42% of its surface, as well as an optimization 4.5 times faster than in [3]. For the bandwidth, the key factor was to identify the sidelobes to be optimized when considering the embedded element model. As for the time reduction, by reducing the optimized area, we got a cost function that is 3.4 times faster.

REFERENCES

[1] C. Fulton, J. Herd, S. Karimkashi, G. Zhang, and D. Zrnic, "Dual-polarization challenges in weather radar requirements for multifunction phased array radar," *2013 IEEE Int. Symp. on Pha. Array Syst. and Tech.*, Waltham, MA, pp. 494-501, 2013.

[2] E. Pottier and L. Ferro-Famil, "Advances in sar polarimetry applications exploiting polarimetric spaceborne sensors," in *Proc. IEEE Radar Conference, RADAR '08*, 2008.

[3] P. Mendes Ruiz, I. Hinostroza, R. Guinvarc'h, and R. L. Haupt, "Size constraint in design of concentric ring array," in *IEEE Int. Symp. on Ant. & Prop. (APSURSI)*, 2015.

[4] J. A. Kaiser, "The archimedean two-wire spiral antenna," *IRE Trans. on Ant. & Prop.*, 8 (3), 312-323, 1960.

[5] R. Guinvarc'h and R. L. Haupt, "Dual polarization interleaved spiral antenna phased array with an octave bandwidth," *IEEE Trans. on Ant. & Prop.*, vol. 58, no. 2, pp. 397-403, 2010.

[6] I. D. Hinostroza Saenz, R. Guinvarc'h, R. L. Haupt, and K. Louertani, "A dual-polarized wideband planar phased array with spiral antennas," *IEEE Trans. on Ant. & Prop.*, vol. 62, no. 9, pp. 4547-4553, 2014.

[7] J. Huang, "A technique for an array to generate circular polarization with linearly polarized elements," *IEEE Trans. Ant. Prop.*, 34(9), 1113-1124, 1986.

[8] P. Mendes Ruiz, I. Hinostroza, R. Guinvarc'h, and R. L. Haupt, "Genetic algorithm optimization of a dual polarized concentric ring array," *2017 Int. Ap. Comp. Elec. Soc. Symp. Italy (ACES)*, Florence, pp. 1-2, 2017.

[9] R. L. Haupt, *Genetic Algorithms in Electromagnetics*. John Wiley & Sons, New Jersey, USA, 2007.